6. J. F. Myrtle, M. R. Haussler, A. W. Norman, *J. Biol. Chem.* **245**, 1190 (1970); E. Kodicek, D. E. M. Lawson, P. W. Wilson, *Nature* **228**, 763 (1970); J. Omdahl *et al.*, in preparation.
7. G. Guroff, H. F. DeLuca, H. Steenbock, *Amer. J. Physiol.* **204**, 833 (1963).
8. T. Suda *et al.*, in preparation.
9. A description of the process, by M. F. Holick and H. F. DeLuca, is in preparation.
10. W. H. Marsh, B. Fingerhut, H. Miller, *Clin. Chem.* **11**, 624 (1965).
11. T. Suda, H. F. DeLuca, H. K. Schnoes, G. Ponchon, Y. Tanaka, M. F. Holick, *Biochemistry* **9**, 2917 (1970).
12. M. F. Holick and H. F. DeLuca, description in preparation.
13. Supported by research grant No. AMO-5800-10 from PHS and by the Harry Steenbock Research Fund of the Department of Biochemistry. I.B. is a Richard Hartenstein fellow and is in receipt of a Wellcome research travel grant.

27 January 1971

X-ray Diffraction Patterns of Transfer RNA Consistent with the Presence of Short Parallel Helices in the Molecule

Abstract. *X-ray diffraction data of yeast formylmethionine transfer RNA,* Escherichia coli *phenylalanine transfer RNA, and* Escherichia coli *arginine transfer RNA single crystals are compared with the Fourier transform of a helix. The results are consistent with the presence of short parallel double helical segments in the transfer RNA molecules.*

Transfer ribonucleic acid (tRNA) molecules play a prominent role in protein biosynthesis. They function as adaptor molecules in the translation of the messenger RNA code into the corresponding polypeptide chain. It is of interest to have information on their molecular structure. Several different models of the tertiary structure of tRNA have been proposed (*1*). All these models are based on the cloverleaf structure of Holley (*2*). These models consist of four main double helical stems, amino acid, dihydrouridine, anticodon, and pseudouridine. We now report x-ray diffraction patterns from single crystals of tRNA which are consistent with the presence of short parallel helices in the molecule.

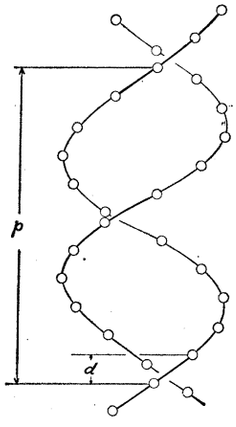

Fig. 1. Elevenfold double helix.

The structural analysis of a macromolecule by single crystal x-ray diffraction can be achieved with the multiple isomorphous derivatives technique. However, although various single crystals of tRNA have been grown and preliminary x-ray diffraction studies have been made (*3*, *4*) deciphering of the phases by the isomorphous derivatives method has not yet been possible. In parallel with our efforts of preparation of the single crystals of heavy atom derivatives, we have attempted to obtain structural information from available diffraction data of the crystals of yeast formylmethionine tRNA ($tRNA^{fMet}$), *Escherichia coli* phenylalanine tRNA ($tRNA^{Phe}$), and *E. coli* arginine tRNA ($tRNA^{Arg}$). X-ray data for these crystals are shown in Table 1.

The two important quantities of a molecular structure that can be compared with the x-ray data are the Fourier transform and the interatomic vector set. We have examined both these quantities and compared them with the x-ray data.

The x-ray diffraction pattern from a crystal is the Fourier transform of all the molecules in the unit cell. Therefore, in general, the diffraction pattern will not directly exhibit the Fourier transform of a single molecule (*5*). However, if the molecule contains a considerable amount of helical structure, the diffraction pattern, may, in favorable cases, be expected to show characteristics of helix diffraction.

The fundamental parameters that define a helix are the pitch p, the number of units per turn N, and the radius r. The distance d between the successive units is then equal to p/N, and the angle of rotation ϕ per unit is equal to $360°/N$ (Fig. 1). The general formula of the Fourier transform of a set of points is

$$F(X,Y,Z) = \sum_j f_j \times \exp\, 2\pi i(Xx_j + Yy_j + Zz_j) \qquad (1)$$

where f_j is the scattering factor of the jth atom whose coordinates are x_j, y_j, and z_j and X, Y, Z are orthogonal coordinates in the reciprocal space. For the infinite helix, Eq. 1 can be written (*6*)

$$F(R,\psi,Z) = \sum_{n=0}^{\infty} J_n(2\pi Rr) \times \exp\, i[n(\psi - \phi + \pi/2) + 2\pi Zz] \qquad (2)$$

where R,ψ,Z are the cylindrical coordinates in the reciprocal space and J_n is the Bessel function of nth order. This function is known to have the following characteristics. (i) The transform has a layer structure, with the distance $1/p$ between the layers; (ii) at the lower layers, the main part of the Bessel function has the same order as the layer number and has a cross-shaped pattern through the origin; (iii) the strong meridional region appears at a distance of about $1/d$; and (iv) for the double helix, the transform is modified by a fringe function corresponding to the relative position of the two strands.

Since the scattering in the low angular region is mainly due to the phosphate group (*7*), the phosphorus coordinates (*8*) of the helix for 11-fold viral RNA with $p = 30$ Å and $N = 11$

Table 1. Crystallographic data for three tRNA crystals.

Species	Crystal system	Space group	Cell constants		Molecules in asymmetric unit (No.)
			$a = b$ (Å)	c (Å)	
Formylmethionine (yeast)	Hexagonal	$P6_222$ ($P6_122$)	115	137	1
Phenylalanine (*E. coli*)	Hexagonal	?	122	198	2(?)
Arginine (*E. coli*)	Trigonal	$P3_121$ ($P3_221$)	99.4	92.9	2

were used in our study. Because the length of the tRNA molecule is finite, the calculations were done with the use of Eq. 1. The characteristics of the transforms of a long and short helix are demonstrated in Fig. 2. Figure 2, a and b, shows the low angular region of the XZ sections of the transforms of an 11-fold double helix of two full turns (22 units) and seven units, respectively. The main features in the transform of the long helix are (i) the layer arrangement and (ii) the cross pattern, similar to those of the infinite helix. However, in the case of the short helix, the layer distribution is less obvious, whereas continuous large values corresponding to the feature (ii) appear in the form of a cross.

The observed weighted reciprocal lattice section XZ is shown for $tRNA^{fMet}$ in Fig. 2c. The highest resolution of this diffraction pattern is 6 Å, and the meridional reflections which are expected around 3 Å were not observed.

A few strong reflections appear along cones with semivertical angles extending from 35° to 45° about the c^* axis. The c axial length is 137 Å, and one period of the helix is 30 Å. Therefore, if the helix is long, strong spots will be expected for layers 4,5,9,13,14,..., along the c^* direction and weak regions in between. However, there is no indication of such a layer arrangement. A similar continuous cross of prominent reflections is also observed in *E. coli* $tRNA^{Phe}$ $0kl$ reciprocal lattice as shown in Fig. 2d. These observations are consistent with the presence of short parallel helical segments in the tRNA molecule.

We now consider the XY section of the transform. The calculated transforms of the XY sections for the long and short helices show similar J_0 type of distribution ($n = 0$ in Eq. 2) with the characteristic concentric rings of alternating strong and weak regions around the origin. The $hk0$ diffraction pattern of $tRNA^{fMet}$ shows a pronounced zero intensity ring of radius

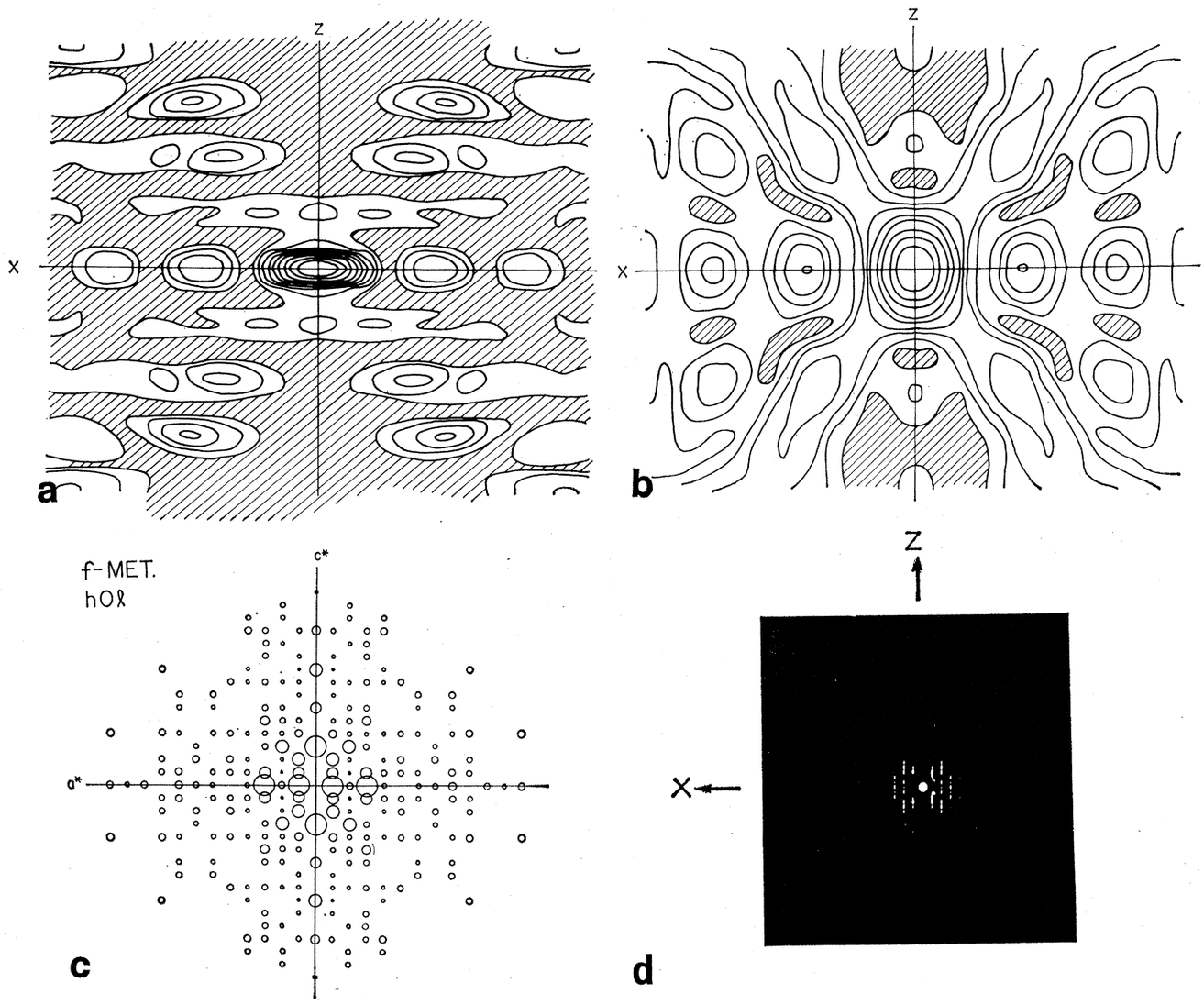

Fig. 2. Fourier transform of a double helix and weighted reciprocal lattice. (a) Amplitude for the XZ section of the transform of the double helix of two full turns. The helix axis is along the Z axis. (b) Amplitude for the XZ section of the transform of the double helix of seven units. (c) The $h0l$ weighted reciprocal lattice of $tRNA^{Met}$. The radius of the circle is proportional to the $|F|$ sharpened by an artificial thermal parameter $B = 100$ Å^2. (d) The $h0l$ diffraction diagram for $tRNA^{Phe}$.

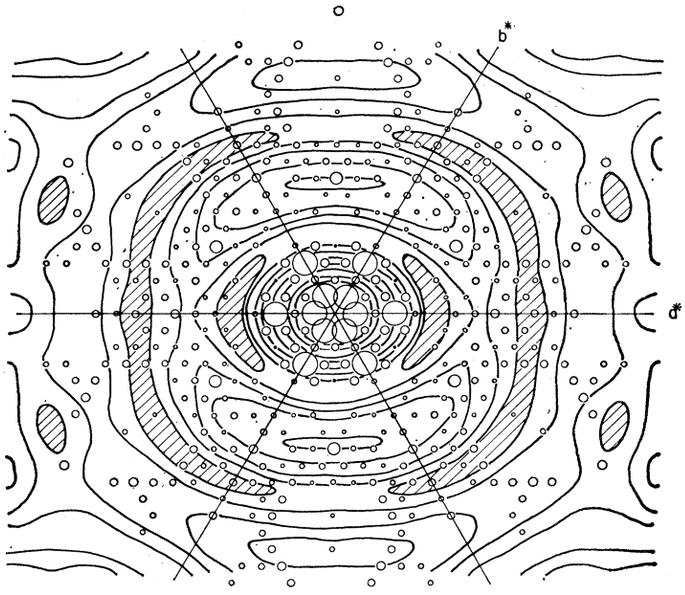

Fig. 3. Superposition of the $hk0$ weighted reciprocal lattice (open circles) of $tRNA^{fMet}$ on the contoured Fourier transform of a double helix of seven units. The lowest regions of the transform are shaded. The first low region of the transform coincides with the low intensities of the weighted reciprocal lattice, whereas the strong intensities coincide with the high regions of the transform. An exact agreement between the two cannot be expected because the molecular Fourier transform is not a complete representation of the weighted reciprocal lattice (*5*).

0.045 to 0.05 per angstrom (Fig. 3).

The zero order Bessel function $J_0(2\pi Rr)$ has its first zero at $2\pi Rr = 2.40$. Therefore, the zero intensity circle corresponds to an r value of 8 to 9 Å, which is in agreement with the radius of the RNA helix for the phosphorus atoms. Thus, the zero intensity circle may also be regarded as indicating the presence of helical structure in the tRNA molecule. The $hk0$ diffraction pattern of *E. coli* $tRNA^{Phe}$ has not yet been obtained to make a similar comparison. In *E. coli* $tRNA^{Arg}$, the $hk0$ and $0kl$ diffraction patterns did not show the characteristics of helical diffraction. This may be attributed to the presence of the two crystallographically independent molecules in different orientations.

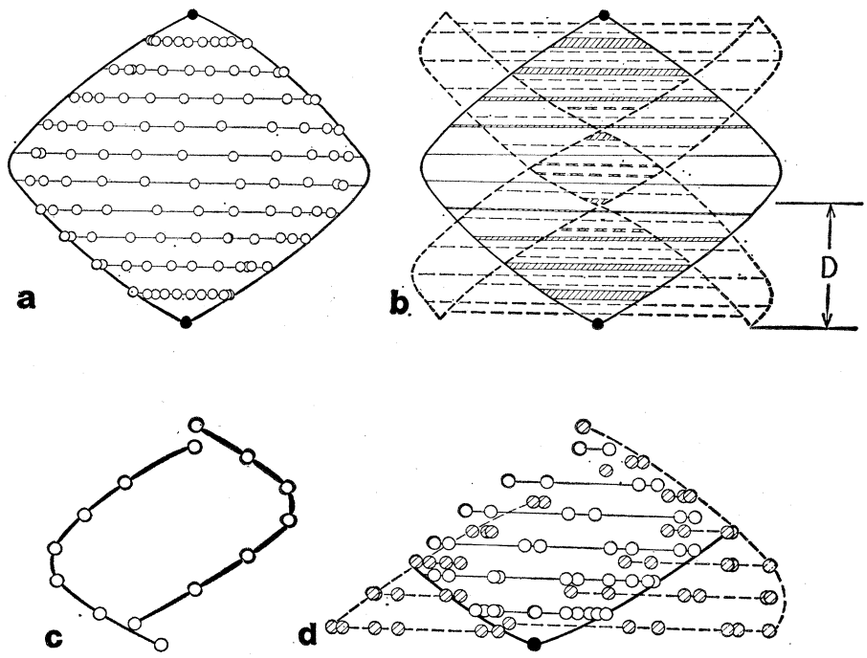

Fig. 4. (a) The vector set of a single helix. Origin is at the black circle. (b) The vector set of a double helix. The solid lines correspond to intrastrand vectors and the dotted lines to the interstrand vectors. The thickness of a layer is roughly proportional to the mean density of points on that circle. Displacement (D) is related to the disposition of the two strands. (c) An 11-fold double helix of seven units. (d) The vector set of a double helix of seven units.

The vector set of a long helix has the following characteristics (Fig. 4a). (i) It consists of parallel layers with spacing d; (ii) the vectors in each layer lie on a circle of radius $2r|\sin(n\phi/2)|$ where n is the layer number. The largest possible radius is twice that of the helix; (iii) the greatest accumulation of vectors is on the z axis (helix axis) at a distance p; and (iv) in the case of double helix, in addition to the above vector set, a similarly shaped interstrand vector set appears, with a displacement D along the z axis (Fig. 4b). If the helix is short (Fig. 4c), the feature (iii) disappears and (iv) is less obvious. This is demonstrated for a helix of seven units in Fig. 4d.

The Patterson map was examined for the features of the vector set listed above. The circles corresponding to the low order layers of the vector set could not be found because they lie within the broad origin peak of the Patterson function. However, no evidence of (iii) and (iv) was found either. This observation is consistent with the earlier conclusion from the study of the Fourier transform that the helical segments are short.

Our studies on two different species of tRNA are consistent with the presence of short parallel helical segments in the molecule. This, taken together with the estimated molecular dimensions (*4*), indicates that the helical segments may be stacked or staggered along the length of the molecule.

After our report was submitted for

publication, we learned that Kim *et al.* have observed x-ray diffraction patterns of yeast $tRNA^{Phe}$ and have interpreted their patterns to be also consistent with the presence of double helical segments, of approximately half a turn, in the molecule (*9*).

T. SAKURAI,* S. T. RAO
J. RUBIN, M. SUNDARALINGAM
Department of Biochemistry, College of Agricultural and Life Sciences, University of Wisconsin, Madison 53706

References and Notes

1. J. Ninio, A. Favre, M. Yaniv, *Nature*, **223**, 1333 (1969); M. Levitt, *ibid.* **224**, 759 (1969); F. Cramer, V. A. Erdmann, F. von der Haar, E. Schlimme, *J. Cell. Physiol.* **74** (Suppl. 1), 163 (1969); G. Melcher, *FEBS Lett.* **3**, 185 (1969); D. J. Abraham, *J. Theor. Biol.* **30**, 83 (1971); P. G. Connors, M. Labanauskas, W. W. Beeman, *Science* **166**, 1528 (1969).
2. R. W. Holley, J. Apgar, G. A. Everett, J. T. Madison, M. Marquisse, S. H. Merrill, J. R. Penswick, A. Zamir, *Science* **147**, 1462 (1965).
3. S. H. Kim and A. Rich, *ibid.* **162**, 1381 (1968); F. Cramer, F. von der Haar, K. C. Holmes, W. Saenger, E. Schlimme, G. E. Schultz, *J. Mol. Biol.* **51**, 523 (1970); B. Vold, *Biochem. Biophys. Res. Commun.* **35**, 222 (1969); M. Labanauskas, P. G. Connors, J. D. Young, R. M. Bock, J. W. Andregg, W. W. Beeman, *Science* **166**, 1530 (1969); J. D. Young, R. M. Bock, S. Nishimura, H. Ishikura, Y. Yamada, U. L. Raj-Bhandary, M. Labanauskas, P. G. Connors, *ibid.* p. 1527; A. Hampel and R. M. Bock, *Biochemistry* **9**, 1873 (1970); C. D. Johnson, K. Adolph, J. J. Rosa, M. D. Hall, P. B. Sigler, *Nature* **226**, 1246 (1970); R. D. Blake, J. R. Fresco, R. Langridge, *ibid.* **225**, 32 (1970); M. Sundaralingam, J. Rubin, S. T. Rao, unpublished work.
4. S. H. Kim and A. Rich, *Science* **166**, 1621 (1969); M. Labanauskas, P. G. Connors, J. D. Young, R. M. Bock, S. T. Rao, M. Sundaralingam, *Abstr. Am. Cryst. Assoc. Winter Meet., New Orleans*, March 1970.
5. This is because the diffraction pattern is a superposition of the Fourier transforms of the molecules related by the crystal symmetry and modulated by the fringe function which depends upon the molecular positions.
6. W. Cochran, F. H. C. Crick, V. Vand, *Acta Cryst.* **5**, 581 (1952).
7. R. Langridge, A. D. Marvin, W. E. Seeds, H. R. Wilson, C. W. Hooper, M. H. F. Wilkins, L. D. Hamilton, *J. Mol. Biol.* **2**, 381 (1960).
8. S. Arnott, M. H. F. Wilkins, W. Fuller, R. Langridge, *ibid.* **27**, 535 (1967); S. Arnott, S. D. Dover, A. J. Wanacott, *Acta Cryst.* **B25**, 2191 (1969).
9. S. H. Kim, C. Quigley, F. L. Suddath, A. Rich, *Proc. Natl. Acad. Sci. U.S.* **68**, 841 (1971).
10. We thank M. Labanauskas for making the $tRNA^{fMet}$ data available to us, Dr. R. McMullan for discussions, and Dr. R. M. Bock and Dr. W. W. Beeman for interest and encouragement. Supported by NIH grant 17378 and NSF grant GP-15977.

* On leave of absence from the Institute of Physical and Chemical Research, Saitama, Japan.

29 March 1971; revised 25 May 1971

Adenosine 3′,5′-Monophosphate Increases Capacity for RNA Synthesis in Rat Liver Nuclei

Abstract. *Liver nuclei isolated from rats injected with adenosine 3′,5′-monophosphate exhibit an increased capacity for RNA synthesis compared with nuclei from control animals. This effect, which is highly specific for the cyclic nucleotide, can be observed within 1 hour after injection in both unoperated and adrenalectomized rats. These findings suggest that induction of enzyme synthesis mediated by way of adenosine 3′,5′-monophosphate may be controlled, at least in part, at the level of gene transcription.*

A wide variety of tissue responses to specific hormones are known to be mediated at the molecular level by adenosine 3′,5′-monophosphate (cyclic AMP), and increased cellular concentrations of cyclic AMP can cause both activation of existing enzymes and induction of the synthesis of new enzymes (*1*). This latter effect could be controlled by actions of cyclic AMP during either translation or transcription, or both.

A possible explanation for effects of cyclic AMP on transcription has recently been reported by Langan (*2, 3*), who has observed that the phosphorylation of histones is stimulated by cyclic AMP. Because histones are thought to usually inhibit gene transcription, it has been postulated that the cyclic AMP–mediated phosphorylation of histones causes them to be displaced from the DNA and thereby allows genes to be transcribed into RNA. Indeed, glucagon, which is known to induce the synthesis of a number of specific enzymes in rat liver, has been found to cause both increased liver concentrations of cyclic AMP and an increase in the phosphorylation of a specific serine residue in F1 histone (*3*). This hypothesis is further supported by the finding that the induction of at least one liver enzyme by glucagon is inhibited by actinomycin D (*4*).

If Langan's hypothesis is correct, then cyclic AMP should cause an increase in the rate of RNA synthesis in rat liver, although the overall effect might not be very great due to the relatively small number of enzymes whose synthesis is induced by this nucleotide. Because it has been shown that the synthesis of specific enzymes can be induced in rat liver by direct administration of cyclic AMP to normal rats (*4, 5*), we decided to determine whether such treatment has any detectable effect on nuclear RNA synthesis. Our experiments show that within 1 hour after administration of cyclic AMP, a dramatic increase occurs in the ability of liver nuclei to synthesize RNA.

Male Sprague-Dawley rats between 150 and 250 g in weight were injected with cyclic AMP (10 mg per 100 g of body weight) or an equivalent volume of saline (0.9 percent NaCl) 1 hour before the animals were killed. Liver nuclei were isolated as a pellet in 2.4*M* sucrose (1 m*M* $MgCl_2$) (*6*), and were incubated in the presence of ^{14}C-labeled adenosine triphosphate (ATP) and unlabeled nucleoside triphosphates to monitor their capacity for RNA synthesis (Table 1). The DNA concentration was determined by the indole method (*7*), and RNA synthesis was expressed as radioactivity incorporated into acid-insoluble material per milligram of DNA.

Although some variability was encountered in different groups of rats, animals injected with cyclic AMP consistently yielded liver nuclei with an in-

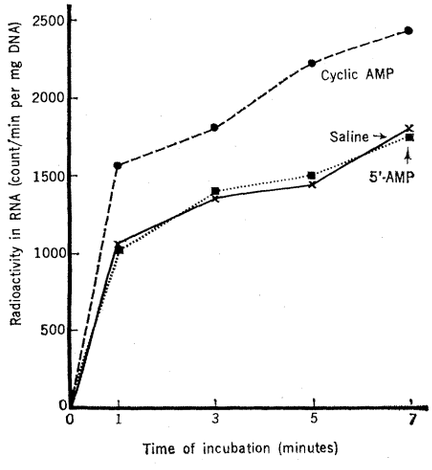

Fig. 1. Time course of RNA synthesis in liver nuclei from rats injected with cyclic AMP, 5′-AMP, or saline (0.9 percent NaCl) 1 hour before the animals were killed. Conditions were those described in Table 1. The stimulation in the rate of RNA synthesis only occurs with cyclic AMP, and the effect is noticeable within the first minute of incubation.